

ANALYSIS OF WAVE FUNCTIONS, ENERGY LEVELS AND CROSS-SECTION FOR (π^+ , K^+) REACTIONS USING NUMEROV'S METHOD

Ye Htet Aung¹, Thi Han², Kyaw Kyaw Naing³, Chit Min Thu⁴, Aung Khant Paing⁵

Abstract

In this paper, the wave functions of single lambda particle for Λ -hypernucleus are calculated by using Numerov's method. And then, the single lambda particle energy levels of various Λ -hypernucleus in Woods-Saxon potential have been studied. Moreover, the single Λ -binding energy and differential cross-section for Λ -hyperon production (π^+ , K^+) reactions of $^{10}_{\Lambda}\text{B}$, $^{12}_{\Lambda}\text{C}$, $^{28}_{\Lambda}\text{Si}$ and $^{89}_{\Lambda}\text{Y}$ have been calculated. The calculated theoretical results of single Λ -binding energy and differential cross-section are well in agreement with the experimental results of KEK. All the numerical calculations are conducted with the help of Fortran-2019 Program.

Keywords: Binding Energy, Differential Cross-section, Fortran2019, Numerov's Method, Λ - hypernucleus, Woods-Saxon Potential

Introduction

A nuclear reaction is a process in which the nucleus of an atom is changed by being split apart or joined with the nucleus of another atom. There are many types of nuclear reaction. But, the (π^+ , K^+) reactions are studied. The single lambda binding energy, energy levels and differential cross-section for (π^+ , K^+) reactions are being gone to study by using phenomenological potential.

The ordinary nucleus consists of protons and neutrons which are subatomic particles called by elementary particles. A hypernucleus is similarly a nucleus but consists of the protons and neutrons in addition to at least one hyperon which is a baryon carrying the strangeness quantum number.[11] Baryon is massive composite hadron which is made up of three quarks and is subdivided into two groups: nucleon and hyperon.

Nucleon consists of a proton and neutron. Hyperon, a strange particle, is larger mass than the nucleon and consisting one or more strange quark and is also called the strange particle. Hyperons are produced by the strong force (about 10^{-23} s) and decayed by the weak force (about 10^{-10} s). There are four kinds of hyperons. They are Lambda (Λ), Sigma (Σ), Xi (Ξ) and Omega (Ω). In 1952, Marian Danysz and Jerzy Pniewski discovered the first nucleus.[14] They used the nuclear emulsion technique, based on their energetic but delayed decay.

Nowadays, lambda particle is interested by scientists in the field of nuclear physics. A product of a proton collision with a nucleus was found to live for much longer time than expected: 10^{-10} s instead of the expected 10^{-23} s in 1947 during a study of cosmic ray interactions. This particle name is lambda (Λ) and the property was dubbed "strangeness" and the name stuck to be the name one of the quarks from which the lambda particle is constructed. The composition of Λ^0 is made up of uds which means up, down and strange quark. The mass of Λ^0 is 1115.683 ± 0.006 MeV/c². The spin of Λ^0 particle is 1/2 and isospin is 0.[13] A lambda particle has been produced with (π^+ , K^+), (K^- , π^-) and (π^- , K^+) reactions. Λ -hyperon does not need to obey Pauli's exclusion principle and can penetrate into the nuclear interior and form deeply bound hypernuclear states.

Aim

The research paper aim is to analyze the energy levels, single lambda binding energy and differential cross-section for (π^+ , K^+) reactions using Numerov's method.

¹ Department of Physics, Defence Services Academy, Pyin Oo Lwin

² Department of Physics, Defence Services Academy, Pyin Oo Lwin

³ Department of Nuclear Physics, Defence Services Academy, Pyin Oo Lwin

⁴ Department of Physics, Defence Services Academy, Pyin Oo Lwin

⁵ Department of Physics, Defence Services Academy, Pyin Oo Lwin

Numerov's Method

Numerov's method was developed by Boris Vasil's Numerov who is the Russian astronomer. The Numerov's method, a numerical method, is used to solve the ordinary differential equation of second order in which the first term does not appear.[7]

The Numerov's method can be used to solve differential equation of the form:

$$\frac{d^2y}{dx^2} = -g(x)y(x) + s(x) \quad (1)$$

The three values of y_{n-1} , y_n , y_{n+1} taken at three equidistant points x_{n-1} , x_n , x_{n+1} are related as follows:

$$y_{n+1} \left(1 + \frac{h^2}{12} g_{n+1} \right) = 2y_n \left(1 - \frac{5h^2}{12} g_n \right) + y_{n-1} \left(1 + \frac{h^2}{12} g_{n-1} \right) + \frac{h^2}{12} (s_{n+1} + 10s_n + s_{n-1}) + o(h^6) \quad (2)$$

Woods-Saxon Potential

The Woods-Saxon potential is used in nuclear physics because it is an important part of understanding the interactions between nucleons (protons and neutrons) inside atomic nuclei. By understanding potential, it can pay insight into the behavior of nucleons, which can help better understand the properties of nuclei, such as binding energy and wave functions. Additionally, the potential can be used to calculate the properties of nuclear reactions and scattering particles of the nuclei.

The Woods-Saxon potential, a mean field potential, is a phenomenological potential used to describe the interaction between nucleons (protons and neutrons) inside an atomic nuclei and is used to describe approximately the forces applied on each nucleon, in the nuclear shell model for the structure of the nucleus. This potential is named after Roger D. Woods and David S. Saxon.[12]

The form of the potential, in terms of the distance r from the center of nucleons is:

$$V(r) = - \frac{V_0}{1 + \exp\left(\frac{r-R}{a}\right)} \quad (3)$$

where, V_0 = the potential well depth

a = the length representing the surface thickness of the nucleus

r = the distance from the center of nucleus

R = the nuclear radius

Numerov's Calculation of Binding Energy and Differential Cross-section for Lambda Single Particle

A transition matrix is a matrix that relates the initial and final states of a physical systems undergoing a transition or scattering process. The transition matrix, a square matrix, describes the probabilities of moving from one state to another in a Markov chain.[10] The transition matrix for the (π^+, K^+) reaction provides a quantitative description of the scattering process. The transition probability per unit time for state ψ_i to ψ_f due to the perturbation can be calculated using the time-independent perturbation theory and is given by:

$$W_{fi} = \frac{2\pi}{\hbar} |T_{fi}|^2 \delta(E_i - E_f) \tag{4}$$

where, T_{fi} = the squared matrix element of the perturbation Hamiltonian between the initial and final state

$E_i - E_f$ = the Dirac delta function that enforces energy conservation

In the ${}^A_Z X(\pi^+, K^+) {}^A_Z X$ reaction, the target nucleus ${}^A_Z X$ is consisted of a neutron and a core nucleus. The incident particle π^+ interacts only with the neutron while the core nucleus remains as a spectator. The elementary process is $\pi^+ + n \rightarrow \Lambda + K^+$, and if the emitted Λ sticks to the core nucleus ${}^A_Z X$ hypernucleus is produced. The schematic diagram of reaction process is as follows;

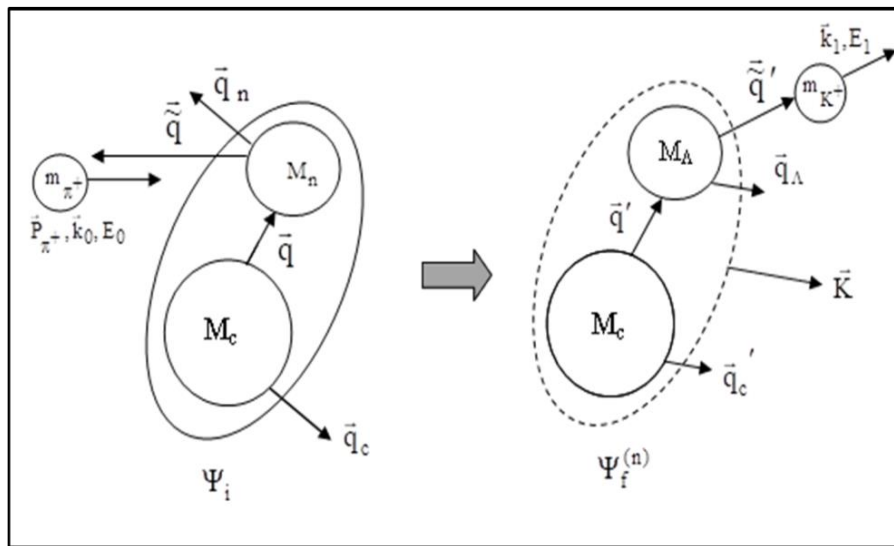


Figure 1. Schematic Diagram of (π^+, K^+) Reaction

The nuclear cross-section in nuclear physics is used to design and optimize nuclear reactor and study the properties of atomic nuclei and develop new nuclear technologies.[9] The differential cross-section is calculated to determine the probability of the various Λ -hyperon production reactions.

$$d^6\sigma = \frac{L^3}{v_0} \frac{2\pi^3}{\hbar} \sum_n \delta(E_i - E_f^{(n)}) \left(\frac{L}{2\pi}\right)^6 d\vec{k}_1 d\vec{k}_2 |T_{fi}^{(n)}|^2 \tag{5}$$

where, $\frac{L^3}{v_0}$ = incident flux

$$v_0 = \frac{\hbar k_0 c^2}{E_0} = \text{incident pion velocity}$$

$$\rho(E) = \left(\frac{L}{2\pi}\right)^3 d\vec{k}_1 \left(\frac{L}{2\pi}\right)^3 d\vec{k}_2 = \text{number of allowed final states}$$

$$\delta(E_i - E_f^{(n)}) = \text{energy conservation term}$$

The differential cross-section for (π^+, K^+) reaction becomes

$$\frac{d^3\sigma}{dE_1 d^2\Omega} = \frac{(2\pi)^4}{\hbar^2 k_{0c}^2} \frac{(\hbar c)^2}{4} |\langle t \rangle_{av}|^2 k_1 - \frac{1}{\pi} \text{Im} \left[\int d\vec{r} d\vec{r}' f^*(\vec{r}) \left\langle \vec{r} \left| \frac{1}{E - H_{\Lambda c} + i\epsilon} \right| \vec{r}' \right\rangle f(\vec{r}') \right] \quad (6)$$

Results and Discussions

In this section, the wave functions, energy levels, single Λ binding energy and differential cross-section will be studied.

Wave Functions for $^{10}\text{B}(\pi^+, \text{K}^+)_{\Lambda}^{10}\text{B}$ Reaction

In this $^{10}\text{B}(\pi^+, \text{K}^+)_{\Lambda}^{10}\text{B}$ reaction, it has two states which are $0s_{1/2}$ and $0p_{3/2}$ state. The wave functions have only positive region. The wave functions of $^{10}\text{B}(\pi^+, \text{K}^+)_{\Lambda}^{10}\text{B}$ reaction are shown in figure (2).

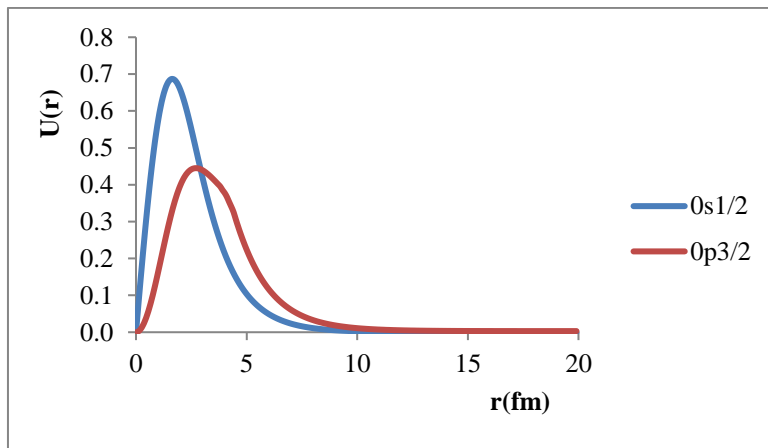


Figure 2. Wave Functions for $^{10}\text{B}(\pi^+, \text{K}^+)_{\Lambda}^{10}\text{B}$ Reaction

Wave Functions for $^{12}\text{C}(\pi^+, \text{K}^+)_{\Lambda}^{12}\text{C}$ Reaction

In this $^{12}\text{C}(\pi^+, \text{K}^+)_{\Lambda}^{12}\text{C}$ reaction, the wave functions have only positive region. The wave functions start increasing from 0 fm. The wave functions for $^{12}\text{C}(\pi^+, \text{K}^+)_{\Lambda}^{12}\text{C}$ reaction are shown in figure 3.

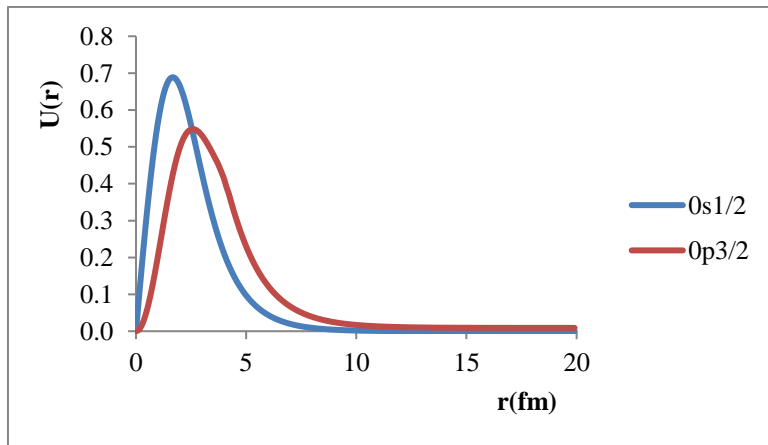


Figure 3. Wave Functions for $^{12}\text{C}(\pi^+, \text{K}^+)_{\Lambda}^{12}\text{C}$ Reaction

Wave Functions for $^{28}\text{Si}(\pi^+, \text{K}^+)_{\Lambda}^{28}\text{Si}$ Reaction

In this $^{28}\text{Si}(\pi^+, \text{K}^+)_{\Lambda}^{28}\text{Si}$ reaction, the four spin states can be found. They are $0s_{1/2}$, $0p_{3/2}$, $0p_{1/2}$ and $0d_{5/2}$ states. The wave functions of $0p_{3/2}$ and $0p_{1/2}$ are nearly identical. The wave functions for $^{28}\text{Si}(\pi^+, \text{K}^+)_{\Lambda}^{28}\text{Si}$ reaction are shown in figure 4.

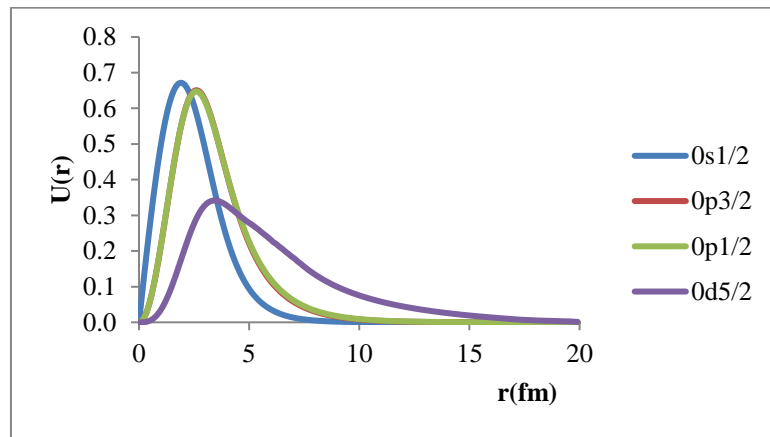


Figure 4. Wave Functions for $^{28}\text{Si}(\pi^+, \text{K}^+)_{\Lambda}^{28}\text{Si}$ Reaction

Wave Functions for $^{89}\text{Y}(\pi^+, \text{K}^+)_{\Lambda}^{89}\text{Y}$ Reaction

The wave functions for $^{89}\text{Y}(\pi^+, \text{K}^+)_{\Lambda}^{89}\text{Y}$ reaction are found positive and negative region which are shown in figure 5. This reaction has $0s_{1/2}$, $0p_{3/2}$, $0p_{1/2}$, $0d_{5/2}$, $1s_{1/2}$, $0d_{3/2}$, $0f_{7/2}$ and $1p_{3/2}$ states. And then, the wave functions of various spin states are found in figure 5.

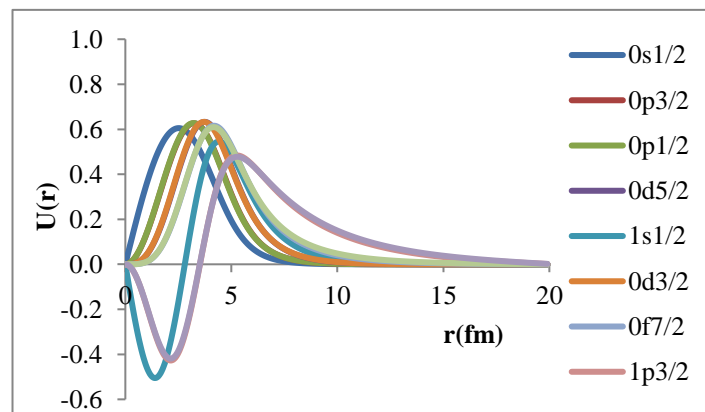


Figure 5. Wave Functions for $^{89}\text{Y}(\pi^+, \text{K}^+)_{\Lambda}^{89}\text{Y}$ Reaction

Lambda Single-particle Energy Levels for Various Hypernuclei

Numerov’s method computes for single-particle energy levels of Woods-Saxon Potential which has analytical result. The numerical calculation results replicate the single-particle energy levels using Woods-Saxon potential which justifies the Numerov’s method to solve the second order differential equation. The results of calculated energy eigen values for single lambda particle using Woods-Saxon potential are shown in figure 6.

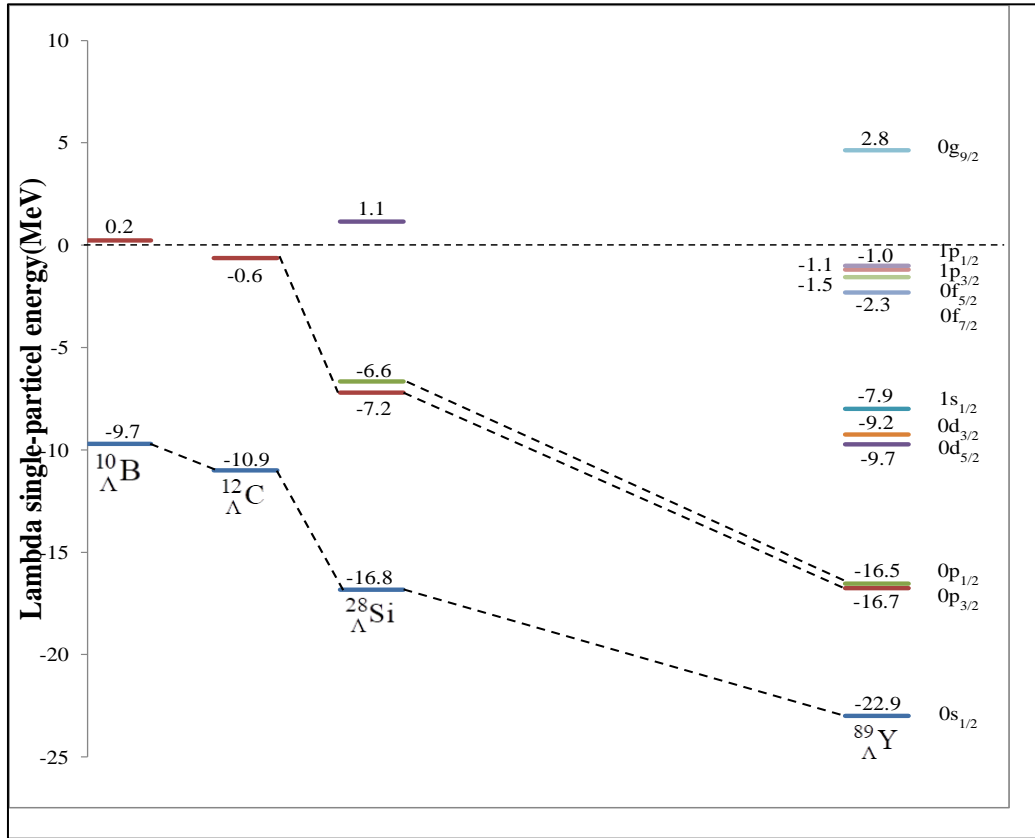


Figure 6. Lambda Single-Particle Energy Levels with Woods-Saxon Potential for Various Hypernuclei

Single Lambda Binding Energy and Differential Cross-section for $^{10}\text{B}(\pi^+, \text{K}^+)_{\Lambda}^{10}\text{B}$ Reaction

In this $^{10}\text{B}(\pi^+, \text{K}^+)_{\Lambda}^{10}\text{B}$ reaction, the two clear peaks of the calculated theoretical spectrum of the Λ -binding energy for $s_{\Lambda}=-9.7$ MeV, $p_{\Lambda}=0.2$ MeV and differential cross-section for $s_{\Lambda}=0.017$ $\mu\text{b}/\text{sr}$, $p_{\Lambda}=0.053$ $\mu\text{b}/\text{sr}$ are shown in figure 7.

The KEK experimental results of the ground state of the single Λ -binding energy at $B_{\Lambda}=-9.1\pm 0.1$ MeV and the excitation state of the single Λ -binding energy at $B_{\Lambda}=0.19\pm 0.2$ MeV and the ground state of the values of differential cross-section at $\sigma=0.017\pm 0.02$ $\mu\text{b}/\text{sr}$ and the excitation state at $\sigma=0.057\pm 0.14$ $\mu\text{b}/\text{sr}$ are shown in figure 8.[6]

The comparison of the theoretical results and the experimental results of KEK for the Λ -binding energy and differential cross-section of $^{10}\text{B}(\pi^+, \text{K}^+)_{\Lambda}^{10}\text{B}$ reaction is shown in table 1. It can be concluded that the theoretical results of Λ -binding energy and differential cross-section are well in agreement with the experimental results of the KEK.

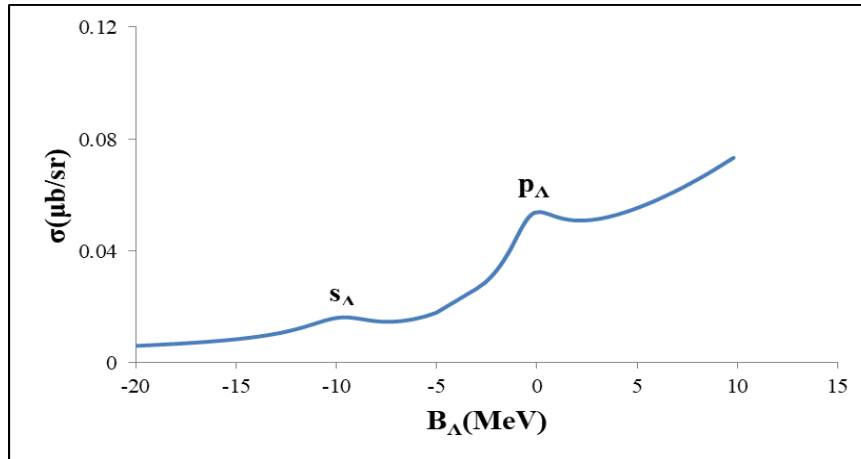


Figure 7. Calculated Results of Single Λ -Binding Energy and Differential Cross-section for $^{10}\text{B}(\pi^+, \text{K}^+)_{\Lambda}^{10}\text{B}$ Reaction

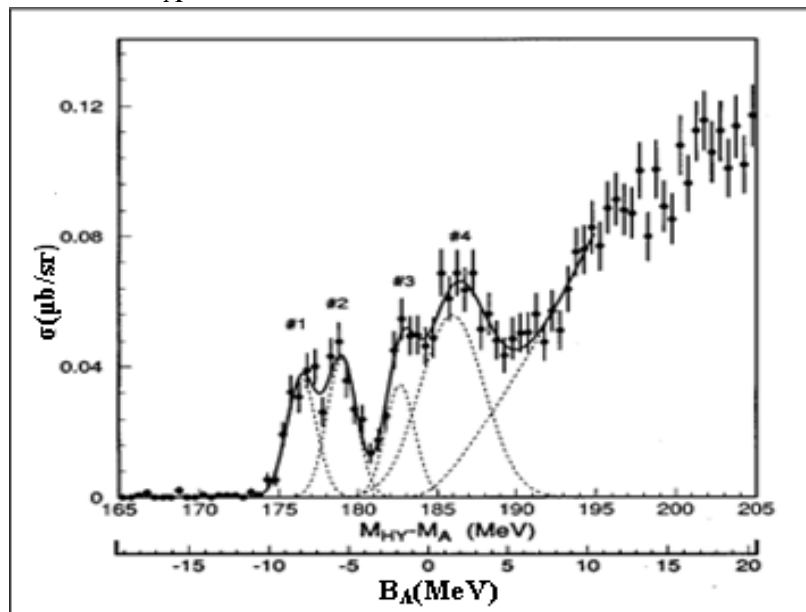


Figure 8. Experimental Results of Single Λ -Binding Energy and Differential Cross-section for $^{10}\text{B}(\pi^+, \text{K}^+)_{\Lambda}^{10}\text{B}$ Reaction.

Table 1. The Comparison with the Calculated Theoretical Results and the Experimental Results of KEK for the Λ -Binding Energy and Differential Cross-section of $^{10}\text{B}(\pi^+, \text{K}^+)_{\Lambda}^{10}\text{B}$ Reaction.

$^{10}\text{B}(\pi^+, \text{K}^+)_{\Lambda}^{10}\text{B}$ Reaction				
	BE(MeV)		Differential Cross-section (σ) ($\mu\text{b}/\text{sr}$)	
Peaks	s_{Λ}	p_{Λ}	s_{Λ}	p_{Λ}
Calculated Results	-9.7	0.2	0.017	0.053
Experimental Results (KEK)[6]	-9.1 ± 0.1	0.19 ± 0.2	0.017 ± 0.2	0.057 ± 0.14

Single Lambda Binding Energy and Differential Cross-section for $^{12}\text{C}(\pi^+, \text{K}^+)_{\Lambda}^{12}\text{C}$ Reaction

In $^{12}\text{C}(\pi^+, \text{K}^+)_{\Lambda}^{12}\text{C}$ reaction, the calculated theoretical spectrum shows the two clear peaks of the Λ -binding energy for $s_{\Lambda} = -10.9$ MeV, $p_{\Lambda} = -0.6$ MeV and differential cross-section for $s_{\Lambda} = 0.166$ $\mu\text{b}/\text{sr}$, $p_{\Lambda} = 0.168$ $\mu\text{b}/\text{sr}$ which are shown in figure 9.

The KEK experimental results of the ground state of the single Λ -binding energy at $B_{\Lambda} = -10.8 \pm 0.1$ MeV and the excitation state of the single Λ -binding energy at $B_{\Lambda} = -0.1 \pm 0.2$ MeV and the ground state of the values of differential cross-section at $\sigma = 0.17 \pm 0.02$ $\mu\text{b}/\text{sr}$ and the excitation state at $\sigma = 0.19 \pm 0.02$ $\mu\text{b}/\text{sr}$ are shown in figure 10.[6]

The comparison with the calculated theoretical results and the experimental results of KEK for the Λ -binding energy and differential cross-section of $^{12}\text{C}(\pi^+, \text{K}^+)_{\Lambda}^{12}\text{C}$ reaction are shown in table 2. The calculated theoretical results of Λ -binding energy and differential cross-section are well in agreement with the experimental results of the KEK.

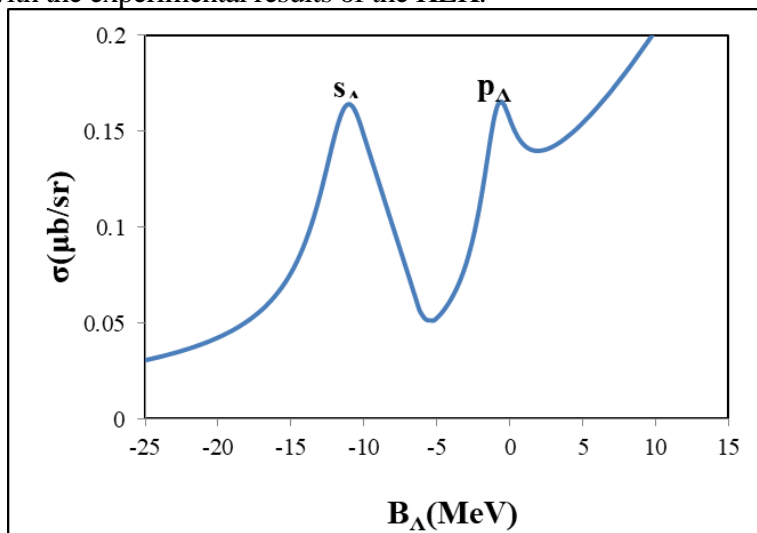


Figure 9. Calculated Results of Single Λ -Binding Energy and Differential Cross-section for $^{12}\text{C}(\pi^+, \text{K}^+)_{\Lambda}^{12}\text{C}$ Reaction

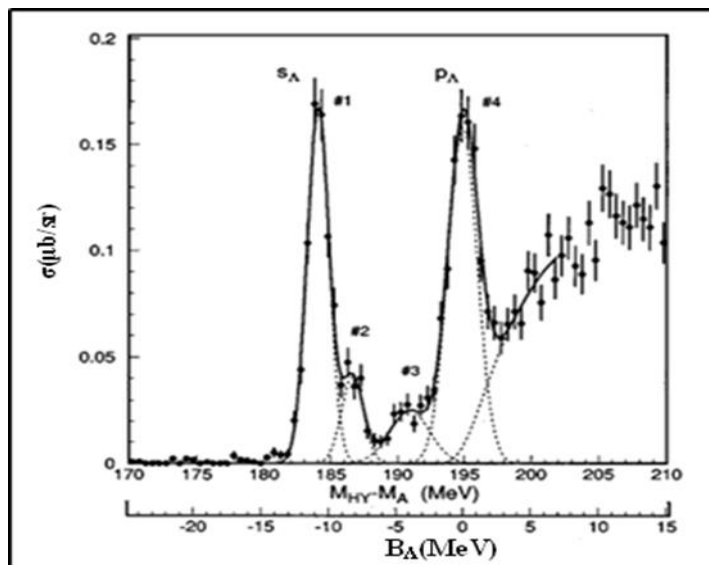


Figure 10. Experimental Results of Single Λ -Binding Energy and Differential Cross-section for $^{12}\text{C}(\pi^+, \text{K}^+)_{\Lambda}^{12}\text{C}$ Reaction

Table 2. The Comparison with the Calculated Theoretical Results and the Experimental Results of KEK for the Λ -Binding Energy and Differential Cross-section of $^{12}\text{C}(\pi^+, \text{K}^+)_{\Lambda}^{12}\text{C}$ Reaction.

$^{12}\text{C}(\pi^+, \text{K}^+)_{\Lambda}^{12}\text{C}$ Reaction				
	BE(MeV)		Differential Cross-section (σ) ($\mu\text{b}/\text{sr}$)	
	s_{Λ}	p_{Λ}	s_{Λ}	p_{Λ}
Peaks	s_{Λ}	p_{Λ}	s_{Λ}	p_{Λ}
Calculated Results	-10.9	-0.6	0.166	0.168
Experimental Results (KEK)[6]	-10.8 ± 0.1	-0.1 ± 0.2	0.17 ± 0.02	0.19 ± 0.02

Single Lambda Binding Energy and Differential Cross-section for $^{28}\text{Si}(\pi^+, \text{K}^+)_{\Lambda}^{28}\text{Si}$ Reaction

In $^{28}\text{Si}(\pi^+, \text{K}^+)_{\Lambda}^{28}\text{Si}$ reaction, the calculated theoretical spectrum shows the two clear peaks of the Λ -binding energy for $s_{\Lambda} = -16.8$ MeV, $p_{\Lambda} = -7.2$ MeV, $d_{\Lambda} = 1.1$ MeV and differential cross-section for $s_{\Lambda} = 0.0138$ $\mu\text{b}/\text{sr}$, $p_{\Lambda} = 0.037$ $\mu\text{b}/\text{sr}$, $d_{\Lambda} = 0.046$ $\mu\text{b}/\text{sr}$ which are shown in figure 11.

The KEK experimental results of the ground state of the single Λ -binding energy at $B_{\Lambda} = -16.6 \pm 0.2$ MeV, -7.0 ± 0.2 MeV and the excitation state of the single Λ -binding energy at $B_{\Lambda} = 1.0 \pm 0.8$ MeV and the ground state of the values of differential cross-section at $\sigma = 0.09 \pm 0.01$ $\mu\text{b}/\text{sr}$, 0.027 ± 0.05 $\mu\text{b}/\text{sr}$ and the excitation state at $\sigma = 0.051 \pm 0.016$ $\mu\text{b}/\text{sr}$ are shown in figure 12.[6]

The comparison with the calculated theoretical results and the experimental results of KEK for the Λ -binding energy and differential cross-section of $^{28}\text{Si}(\pi^+, \text{K}^+)_{\Lambda}^{28}\text{Si}$ reaction are shown in table 3. The calculated theoretical results of Λ -binding energy and differential cross-section are well in agreement with the experimental results of the KEK.

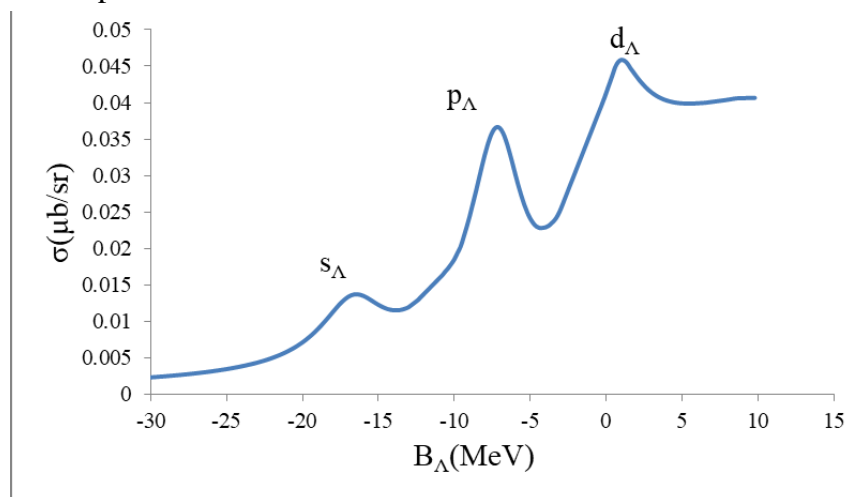


Figure 11. Calculated Results of Single Λ -Binding Energy and Differential Cross-section for $^{28}\text{Si}(\pi^+, \text{K}^+)_{\Lambda}^{28}\text{Si}$ Reaction

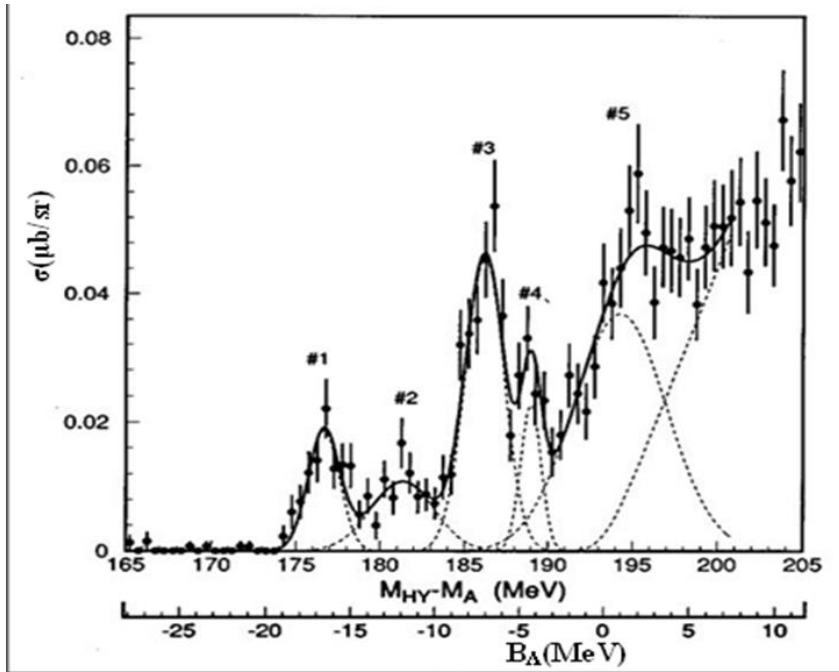


Figure 12. Experimental Results of Single Λ -Binding Energy and Differential Cross-section for $^{28}\text{Si}(\pi^+, K^+)_{\Lambda}^{28}\text{Si}$ Reaction.

Table 3. The Comparison with the Calculated Theoretical Results and the Experimental Results of KEK for the Λ -Binding Energy and Differential Cross-section of $^{28}\text{Si}(\pi^+, K^+)_{\Lambda}^{28}\text{Si}$ Reaction.

$^{28}\text{Si}(\pi^+, K^+)_{\Lambda}^{28}\text{Si}$ Reaction						
Peaks	BE(MeV)			Differential Cross-section (σ) ($\mu\text{b}/\text{sr}$)		
	s_{Λ}	p_{Λ}	d_{Λ}	s_{Λ}	p_{Λ}	d_{Λ}
Calculated Results	-16.8	-7.2	1.1	0.0138	0.037	0.046
Experimental Results (KEK)[6]	-16.6 ± 0.2	-7.0 ± 0.2	1.0 ± 0.2	0.009 ± 0.01	0.027 ± 0.05	0.051 ± 0.016

Single Lambda Binding Energy and Differential Cross-section for $^{89}\text{Y}(\pi^+, K^+)_{\Lambda}^{89}\text{Y}$ Reaction

In $^{89}\text{Y}(\pi^+, K^+)_{\Lambda}^{89}\text{Y}$ reaction, the calculated theoretical spectrum shows the two clear peaks of the Λ -binding energy for $s_{\Lambda} = -22.99$ MeV, $p_{\Lambda} = -16.75$ MeV, $d_{\Lambda} = -9.72$ MeV, $f_{\Lambda} = -2.31$ MeV and differential cross-section for $s_{\Lambda} = 0.0078$ $\mu\text{b}/\text{sr}$, $p_{\Lambda} = 0.0409$ $\mu\text{b}/\text{sr}$, $d_{\Lambda} = 0.117$ $\mu\text{b}/\text{sr}$, $f_{\Lambda} = 0.141$ $\mu\text{b}/\text{sr}$ which are shown in figure 13.

The KEK experimental results of the ground state of the single Λ -binding energy at $B_{\Lambda} = -22.0 \pm 0.5$ MeV, -16.1 ± 0.3 MeV, -9.3 ± 0.4 MeV, -2.3 ± 0.3 MeV and the values of differential cross-section at $\sigma = 0.008 \pm 0.005$ $\mu\text{b}/\text{sr}$, 0.04 ± 0.01 $\mu\text{b}/\text{sr}$, 0.13 ± 0.04 $\mu\text{b}/\text{sr}$, 0.138 ± 0.05 $\mu\text{b}/\text{sr}$ are shown in figure 14.[6]

The comparison with the calculated theoretical results and the experimental results of KEK for the Λ -binding energy and differential cross-section of $^{89}\text{Y}(\pi^+, \text{K}^+)_{\Lambda}^{89}\text{Y}$ reaction are shown in table 4. The calculated theoretical results of Λ -binding energy and differential cross-section are well in agreement with the experimental results of the KEK.

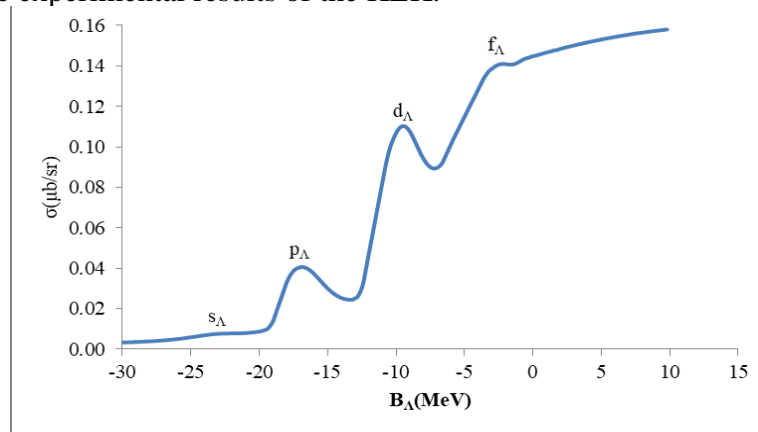


Figure 13. Calculated Results of Single Λ -Binding Energy and Differential Cross-section for $^{89}\text{Y}(\pi^+, \text{K}^+)_{\Lambda}^{89}\text{Y}$ Reaction

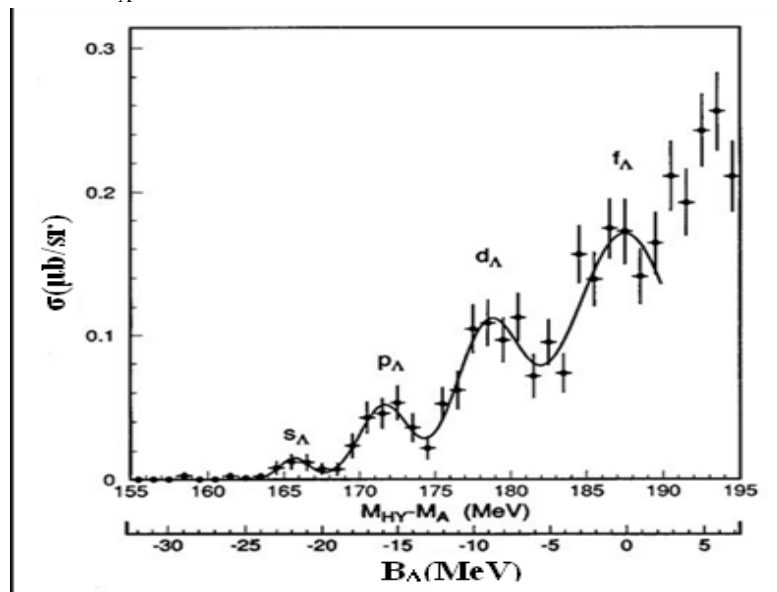


Figure 14. Experimental Results of Single Λ -Binding Energy and Differential Cross-section for $^{89}\text{Y}(\pi^+, \text{K}^+)_{\Lambda}^{89}\text{Y}$ Reaction

Table 4. The Comparison with the Calculated Theoretical Results and the Experimental Results of KEK for the Λ -Binding Energy and Differential Cross-section of $^{89}\text{Y}(\pi^+, \text{K}^+)_{\Lambda}^{89}\text{Y}$ Reaction.

$^{89}\text{Y}(\pi^+, \text{K}^+)_{\Lambda}^{89}\text{Y}$ Reaction				
State	BE(MeV)		Differential Cross-section (σ) ($\mu\text{b}/\text{sr}$)	
	Calculated Results (MeV)	KEK Experimental Results (MeV)[6]	Calculated Results ($\mu\text{b}/\text{sr}$)	KEK Experimental Results ($\mu\text{b}/\text{sr}$) [6]
s_{Λ}	-22.99	-22.0 ± 0.5	0.0078	0.008 ± 0.005
p_{Λ}	-16.75	-16.1 ± 0.3	0.0409	0.04 ± 0.01
d_{Λ}	-9.72	-9.3 ± 0.4	0.117	0.13 ± 0.04
f_{Λ}	-2.31	-2.3 ± 0.3	0.141	0.138 ± 0.05

Conclusion

In this paper, the single lambda energy levels of Λ -hypernuclei have been analyzed. The two-body Schrödinger equation of second order differential form is solved by Numerov's Method and Taylor Series. The energy eigen values for various spin states are carried out by using Fortran-2019 program. Moreover, the energy levels diagrams for ${}^{10}_{\Lambda}\text{B}$, ${}^{12}_{\Lambda}\text{C}$, ${}^{28}_{\Lambda}\text{Si}$ and ${}^{89}_{\Lambda}\text{Y}$ have been computed using Woods-Saxon potential. It is found that the more nuclear mass number, the less lambda single-particle energies in Λ -hypernucleus. Furthermore, it can be concluded that the calculated theoretical results of Λ -binding energy and differential cross-section are well in agreement with the experimental results of KEK.

Acknowledgements

I would like to express my deeply thanks to Dr Kyaw Kyaw Naing, my respectable teacher in DSA, because of helping me throughout this research paper and Dean of Faculty of Physics and Head of Physics Department of Defence Services Academy because of giving opportunity to read this paper in MAAS 2023.

References

- Amaku M., Coutinho F. A. B. and Toyama F. M., "The Normalization of Wavefunctions of the Continuous Spectrum" August 17, 2019.
- Amsler, C; et al., "Review of Particle Physics" 2008.
- Ananthanarayan, B. and Shayan Ghosh , "Pion Interactions and the Standard Model at High Precision" Centre for High Energy Physics, December, 2018.
- Boyer, C. and Merzbach, U., "A History of Mathematics", 1991.
- Daniel Schroeder V., "The Radial Equation", January, 2022.
- Hasegawa, T; et al; "Spectroscopic Study of ${}^{10}_{\Lambda}\text{B}$, ${}^{12}_{\Lambda}\text{C}$, ${}^{28}_{\Lambda}\text{Si}$, ${}^{89}_{\Lambda}\text{Y}$, ${}^{139}_{\Lambda}\text{La}$ and ${}^{208}_{\Lambda}\text{Pb}$ by the (π^+, K^+) Reactions", March, 1996.
- Herbert Goldstein, Charles P. Pille, JR. and John L. Safko, "Classical Mechanics", Third Edition, 2000.
- Hervé Abdi, "The Eigen-Decomposition: Eigenvalues and Eigenvectors", 2007.
- Jackson, C. D., "Classical Electrodynamics", John Wiley and Sons, 1962.
- Povh, B., "Hyperon in Nuclei", May, 1976.
- Schierz, N., Wiedenhover, I. and Volya, A., "Parameterization of the Woods-Saxon Potential for Shell-Model Calculations", 2007.
- Wasserman Eric, W., "Eigenfunction", 2016.
- Zyla, P.A; et al., "Review of Particle Physics", 2020.